Smectic Membranes in Motion: Approaching the Fast Limits of X-Ray Photon Correlation Spectroscopy

Irakli Sikharulidze,[1] Igor P. Dolbnya,[2] Andrea Fera,[1] Anders Madsen,[3]
Boris I. Ostrovskii,[1,4] and Wim H. de Jeu[1]

[1]*FOM Institute for Atomic and Molecular Physics, Kruislaan 407, 1098 SJ Amsterdam, The Netherlands*
[2]*DUBBLE CRG, ESRF, BP 220, 38043 Grenoble, France*
[3]*ID10A, ESRF, BP 220, 38043 Grenoble, France*
[4]*Institute of Crystallography, Academy of Sciences of Russia, Leninsky prospect 59, 117333 Moscow, Russia*

(Received 18 September 2001; published 28 February 2002)

The dynamics of the layer-displacement fluctuations in smectic membranes have been studied by x-ray photon correlation spectroscopy (XPCS). We report transitions from an oscillatory damping regime to simple exponential decay of the fluctuations, both as a function of membrane thickness and upon changing from specular to off-specular scattering. This behavior is in agreement with recent theories. Employing avalanche photodiode detectors and the uniform filling mode of the synchrotron storage ring, the fast limits of XPCS have been explored down to 50 ns.

DOI: 10.1103/PhysRevLett.88.115503 PACS numbers: 61.30.–v, 42.25.Kb, 61.10.Kw

If coherent radiation is incident on a material, the scattered intensity shows a so-called speckle pattern that reflects the instantaneous spatial arrangement of the scatterers. Information about the dynamics of the scatterers is accessible by photon correlation spectroscopy (dynamic light scattering), in which the time dependent intensity autocorrelation function of the speckle pattern is measured. While this is a well-established technique for visible laser light [1], in the x-ray regime the required coherent x-ray intensity can only be generated at third generation high-brilliance synchrotron sources [2]. So far, the feasibility of x-ray photon correlation spectroscopy (XPCS) has been shown on various hard [3] and soft condensed matter systems, including capillary waves at liquid surfaces [4]. Applications to smectic membranes are more recent [5,6]. Smectic liquid crystals consist of stacks of liquid layers, each consisting of orientationally ordered elongated molecules. The reduced dimensionality associated with the density modulation along the layer normal leads to strong thermal fluctuations: the layer displacements $\langle u^2(\mathbf{r})\rangle$ diverge logarithmically with the size of the system (Landau-Peierls instability) [7]. Smectic liquid crystals can be suspended over an opening in a solid frame [8]. The surface area of such a smectic membrane can be as large as several cm^2, while the thickness can be varied from thousands of layers (tens of μm) down to two layers (about 5 nm). Smectic membranes constitute ideal model systems to investigate fundamental aspects of fluctuations associated with low-dimensional ordering. This is directly related to the general interest in surface ordering in systems such as Langmuir films, Newtonian black films, and surfactant and lipid membranes [7,9]. We report on transitions from oscillatory to exponential decay of the fluctuations, both as a function of membrane thickness and of the wave vector transfer along the membrane. Moreover, we have pushed the time scale of XPCS down to well below the μs range (first measurement points at 50 ns). This nicely creates overlap with neutron spin-echo methods that can be extended up to about 100 ns.

Significant progress has been made in both the static [10] and the dynamic [11,12] description of fluctuations in smectic membranes by extending the Landau–de Gennes theory of smectic-*A* (Sm-*A*) with surface terms. Because of the finite film thickness the continuous bulk response spectrum changes into discrete response modes. In contrast to (surface) capillary waves the fluctuations originate from the stacked layers as a whole. Extensive experiments on smectic membranes have been conducted using static x-ray scattering [13,14]. A first series of XPCS measurements with soft x rays on 5–50 μm thick membranes revealed an exponential decay of the correlation function [5]. For different materials a linear dependence between the relaxation time and the membrane thickness was established. In contrast, Fera *et al.* [6], using XPCS with 8 keV x rays, found oscillatory damping in thin membranes. The conditions under which these two situations occur have so far not been established experimentally.

We have studied the compounds N-(4-*n*-butoxybenzilidene)-4-*n*-octylaniline (4O.8) and 4-heptyl-2-[4-(2-perfluorhexylethyl)phenyl]-pyrimidin (FPP) (see Fig. 1),

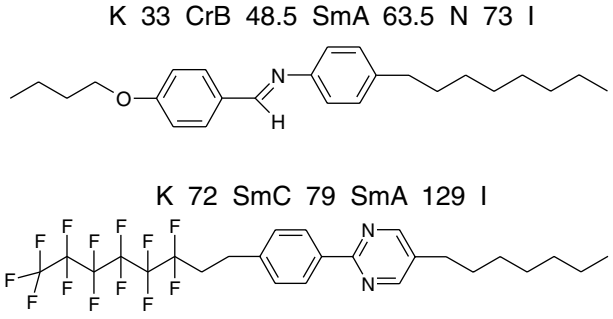

FIG. 1. Compounds: 4O.8 (up) [6] and FPP (down) [14]. Phase transition temperatures are given in °C.

of which FPP has somewhat atypical material parameters such as an unusually large compressibility constant. Membranes were stretched to a size of about 15×5 mm^2 using a frame with movable blades. The frame was placed inside a two-stage oven controlled within 0.1 °C, which was subsequently evacuated. All measurements were done in the Sm-*A* phase at $T = 50$ °C for 4O.8 and $T = 100$ °C for FPP. Membrane thicknesses in a range of 0.5–20 μm were determined from optical reflectometry [8] and up to 3 μm from the interference fringes measured by specular x-ray reflectivity.

X-ray scattering experiments were performed at the undulator beam line ID10A (Troika I) of the European Synchrotron Radiation Facility (ESRF, Grenoble). Membranes were mounted vertically in a reflection geometry (see inset Fig. 2) and illuminated with 8 keV radiation selected by a Si(111) monochromator followed by Pt coated Si mirror to suppress higher harmonics. The longitudinal coherence length of about 1.5 μm is fixed by the bandpass of the monochromator $\Delta\lambda/\lambda \approx 10^{-4}$. The beam emerging from three undulators in series was collimated by a system of two slits and focused in the vertical direction by a refractive beryllium lens with a demagnification ratio of ~1:1. This symmetrizes the transversal coherence lengths to about 10 μm, the same size as the 10 μm pinhole in front of the sample. Guard slits were placed after the pinhole to remove parasitic scattering. The footprint of the beam at the Bragg position was about 0.01×0.5 mm^2. A fast avalanche photodiode (Perkin Elmer C30703) [15] with an intrinsic time resolution $\lesssim$4 ns was used as a detector at a distance of 1.5 m from the sample, with predetector slits set to 30×30 μm^2. The resolution of the setup is estimated to be $\Delta q_x \approx 10^{-4}$ nm^{-1} and $\Delta q_y = \Delta q_z \approx 10^{-3}$ nm^{-1}. Measurements were performed in the 16-bunch mode of the storage ring (16 narrow electron bunches equally spaced at 176 ns time intervals) and in the uniform filling mode (992 bunches at intervals of 2.8 ns). The coherent photon intensity at the sample was about 6×10^8 counts s^{-1}/100 mA. Depending on the mode the intensity time autocorrelation function was computed in real time using a hardware multiple-tau digital autocorrelator ALV5000/E (ALV-GmbH, sampling/lag time down to 200 ns) or with an ALV5000/FAST (sampling intervals down to 12.5 ns). In practice, the technical cutoff of the whole detection tract with the FAST correlator was at 40–50 ns. Ultimately the time structure of the storage ring limits the fastest accessible dynamics. We worked at the Bragg position corresponding to the smectic layer spacing d. Thanks to the perfect match between the millidegree mosaicity of the membranes (see inset in Fig. 3) and the high resolution of the setup, count rates up to 150 MHz were possible. This facilitated measurements at off-specular positions ($q_x \neq 0$) by rocking the sample.

Figure 2 shows correlation functions $g_2(\tau) = \langle I(t+\tau)I(t)\rangle/\langle I(t)\rangle^2$ for 4O.8 membranes in the Sm-*A* phase for various thicknesses. The correlation functions are normalized to the correlation function of the primary beam. Clearly the oscillations become less pronounced and finally disappear with increasing membrane thickness. We did not observe such a crossover for FPP membranes up

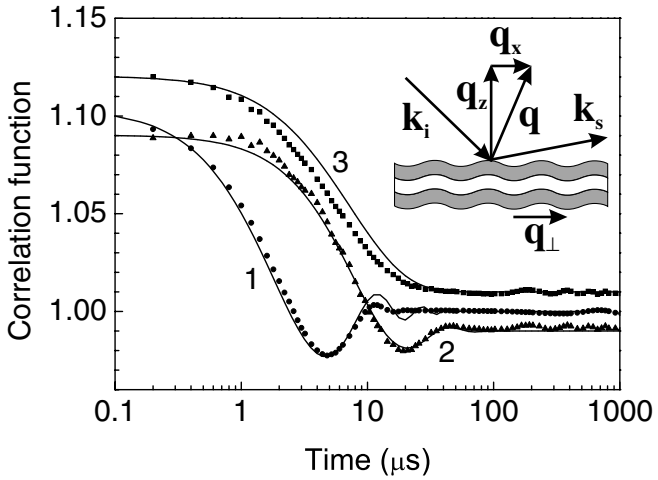

FIG. 2. Autocorrelation function of 4O.8 membranes at the specular position $q_z = 2.2$ nm^{-1} ($d = 2.86$ nm). Circles show data for a 0.3 μm, triangles for a 4.0 μm, and squares for a 7.0 μm thick membrane. Solid lines are fits with parameters [6] $\gamma = 0.021$ N/m, $\eta_3 = 0.05$ kg m^{-1} s^{-1}, $\rho_0 = 10^3$ kg/m^3. Furthermore $\Delta q_x = 5 \times 10^{-5}$ nm^{-1} and Λ values are 180 μm, 160 μm, and 50 μm for curves 1, 2, and 3, respectively. Curves 2 and 3 have been shifted by ± 0.01 for clarity. Inset: Scattering geometry. $\mathbf{k}_i$ and $\mathbf{k}_s$ represent the incident and scattered wave vector, respectively, $|\mathbf{k}_s| = |\mathbf{k}_i|$ and $\mathbf{q} = \mathbf{k}_s - \mathbf{k}_i$. $\mathbf{q}_\perp$ represents a wave vector of the layer undulations.

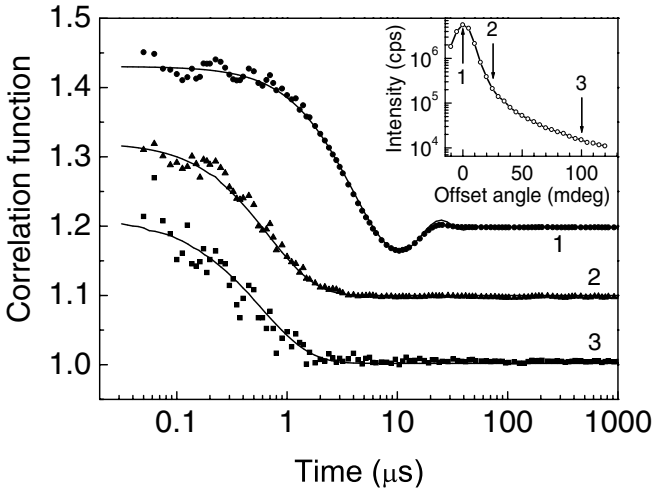

FIG. 3. Autocorrelation functions of a 2.83 μm thick FPP membrane at $q_z = 2.18$ nm^{-1} ($d = 2.94$ nm). Circles show data at $q_x = 0$ (specular), triangles at an offset $q_x = 0.95 \times 10^{-3}$ nm^{-1}, and squares at $q_x = 3.8 \times 10^{-3}$ nm^{-1}. Solid lines are fits with parameters [14] $\gamma = 0.013$ N/m, $\eta_3 = 0.015$ kg m^{-1} s^{-1}, $\rho_0 = 10^3$ kg/m^3. Furthermore $\Delta q_x = 9 \times 10^{-5}$ nm^{-1} and $\Lambda = 90$ μm. Curves 1 and 2 have been shifted by 0.1 and 0.2, respectively. Inset: rocking curve.

to the largest thickness (15 μm) reached experimentally. Figure 3 shows a series of off-specular measurements of this compound. Only the data at the specular ridge (curve 1) show oscillatory behavior. Even for the smallest offset in q_x, corresponding to 0.025°, the oscillatory behavior disappears. Also the relaxation times have moved to values well below 1 μs.

The results will be compared with the theory of fluctuations in Sm-A membranes [11]. The calculations are based on the solution of the equation of motion for such membranes:

$$\rho_0 \frac{\partial^2 u(\mathbf{r})}{\partial t^2} = \eta_3 \frac{\partial}{\partial t} \nabla_\perp^2 u(\mathbf{r}) + (B\nabla_z^2 - K\Delta_\perp^2) u(\mathbf{r}), \quad (1)$$

with corresponding boundary conditions at $z = \pm L/2$ incorporating the surface tension γ. Here ρ_0 is the density, η_3 is the layer shear viscosity coefficient, L is the thickness of the membrane and K and B are the elastic constants corresponding to layer bending and compression, respectively. The experimental $g_2(t)$ have been fitted to the expression $CS^2(\mathbf{q}, t) + O$, where C and O are constants indicating contrast and offset. $S(\mathbf{q}, t)$ is the intermediate scattering function given by

$$S(\mathbf{q}, t) = \int_0^\infty \int_0^\infty dx\, dy \cos(q_x x) \cos(q_y y) \exp\left[-\frac{1}{2} (\Delta q_x x)^2 \right] \exp\left[-\frac{1}{2} (\Delta q_y y)^2 \right] \exp\left[-\frac{1}{2} q_z^2 g(r_\perp, t) \right], \quad (2)$$

where (x, y) is the surface plane of the membrane, $g(r_\perp, t)$ is the layer displacement autocorrelation function (see below), and $r_\perp = \sqrt{x^2 + y^2}$. As the resolution Δq_y is an order of magnitude larger than Δq_x, we can approximate the corresponding exponential by a δ function reducing the integration in Eq. (2) to the x direction only. In high-compressibility limit ($B \to \infty$) the expression for $g(r_\perp, t)$ is given by [11]

$$g(r_\perp, t) = \langle [u(0,0) - u(r_\perp, t)]^2 \rangle = \frac{1}{\pi} \int_{2\pi/\Lambda}^{2\pi/a} dq_\perp\, q_\perp [G(q_\perp, 0) - J_0(r_\perp q_\perp) G(q_\perp, t)], \quad (3)$$

where the correlation function $G(q_\perp, t) = \langle u^*(q_\perp, 0) u(q_\perp, t) \rangle$ has the following form:

$$G(q_\perp, t) = \frac{k_B T \tau_1 \tau_2}{L\rho_0(\tau_1 - \tau_2)} \left[\tau_1 \exp\left(-\frac{|t|}{\tau_1} \right) - \tau_2 \exp\left(-\frac{|t|}{\tau_2} \right) \right], \quad (4)$$

where $k_B T$ is the Boltzmann factor. The times τ_1 and τ_2 are determined by the dispersion relation [11]:

$$\tau_{1,2} \approx \frac{2\rho_0}{\eta_3 q_\perp^2} \left(1 \mp \sqrt{1 - \frac{8\rho_0 \gamma}{q_\perp^2 \eta_3^2 L}} \right)^{-1}. \quad (5)$$

The corresponding relaxation times, given by $[\mathrm{Re}(1/\tau_1)]^{-1}$ and $[\mathrm{Re}(1/\tau_2)]^{-1}$, are displayed in Fig. 4. For small values of $q_\perp$, τ_1 and τ_2 are complex conjugate numbers and both relaxation times coincide, which implies oscillatory damping (complex mode). If $q_\perp$ exceeds a crossover value $q_{\perp,c}$, τ_1 and τ_2 are different real numbers corresponding to a slow and a fast relaxation. In this regime the correlation function follows a simple exponential decay. From Eq. (5) we find

$$q_{\perp,c} \approx \frac{2}{\eta_3} \sqrt{\frac{2\rho_0 \gamma}{L}}. \quad (6)$$

The fast relaxation τ_2 is related to the presence of the inertia term in the equation of motion (1). According to Fig. 4 this relaxation time goes rapidly down with increasing $q_\perp$ and will not be accessible experimentally.

The correlation function (3) represents a superposition of contributions from undulations with different wave vectors. The short-wavelength cutoff in Eq. (3) is defined by the intermolecular distance a, taken as 0.4 nm. The long-wavelength cutoff Λ influences both the damping time and the form of the correlation function. The longest wavelength in a finite-size membrane is determined by the size of the frame. However, in our x-ray experiments the largest wavelength detected would rather be determined by the projection of the coherence length at a given q_z position. In our fitting of the experimental curves the cutoff Λ was varied around 100 μm, which is compatible to the latter interpretation. Fluctuations with larger wavelengths could, nevertheless, still be important as they also disturb the position of the scatterers. A proper implementation of

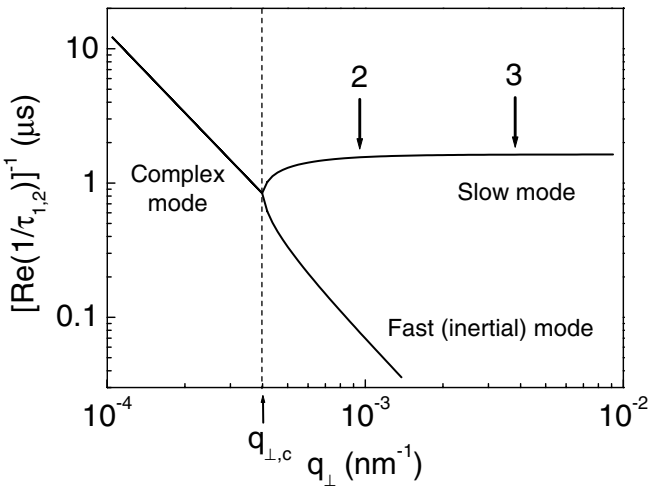

FIG. 4. Calculation of the relaxation times for the FPP membrane presented in Fig. 3. The arrows correspond to the off-specular positions of curve 2 and 3 from Fig. 3.

the coherence and the resolution in the theory would probably introduce some weight function in Eq. (3), which would suppress the contribution of the longer wavelengths more smoothly.

If the crossover wave vector $q_{\perp,c}$ is within the integration interval of Eq. (3), the correlation function exhibits oscillatory damping. As soon as $q_{\perp,c}$ is outside this integration interval an exponential decay is observed. As $q_{\perp,c}$ scales with the membrane thickness as $1/\sqrt{L}$ we can translate this behavior into a cutoff membrane thickness:

$$L_c = \frac{2\rho_0\gamma}{\pi^2\eta_3^2}\,\Lambda^2. \tag{7}$$

For membranes with $L < L_c$ oscillatory behavior will be pronounced. When the membrane thickness approaches L_c the oscillations start to vanish and for $L > L_c$ only an exponential decay is observed. This is in agreement with the results for 4O.8 membranes presented in Fig. 2. For FPP the viscosity η_3 as determined from the fits, is a factor of 3 smaller than for 4O.8 (compare Figs. 2 and 3). Then L_c is for FPP an order of magnitude larger than for 4O.8 and outside our experimental range of thicknesses.

In agreement with surface light scattering methods [9], by rocking the sample to an off-specular angle we probe relaxations with the corresponding wave vector $q_\perp$. Such results for FPP are presented in Fig. 3. The relaxation times corresponding to curves 2 and 3 are almost identical, in agreement with the plateau region in Fig. 4. Larger offset positions could not be measured because of the rapidly decreasing count rate. Note that Eqs. (2) and (3) do not provide a direct relation between the experimental value of q_x and the dominating fluctuation $q_\perp$. This makes a direct quantitative comparison of Figs. 3 and 4 inappropriate. Nevertheless, the difference of approximately a factor 2 between the observed relaxation time and $\mathrm{Re}(1/\tau_1)^{-1}$ from Fig. 4, common in a homodyne detection scheme, suggests that $g_2(t)$ might be represented by a simple exponential. Such a phenomenological form of the correlation function has been used previously to fit experimental data [5,6].

In conclusion, we have measured relaxation times well below 1 μs with data points starting at 50 ns. In principle this number can be pushed down by another order of magnitude to a few ns, the present limit given by the bunch structure of the storage ring. We have found a crossover between an oscillatory and an exponential regime of fluctuation damping, both as a function of membrane thickness and of the off-specular wave-vector transfer. The results are in a good agreement with present theories.

The authors wish to thank G. Grübel (ESRF) for his support at beam line ID10A, and A. Shalaginov for theoretical discussions. This work is part of the research program of the "Stichting voor Fundamenteel Onderzoek der Materie" (FOM), which is financially supported by the "Netherlandse Organisatie voor Wetenschappelijk Onderzoek" (NWO). B. I. O. acknowledges support from NWO in the framework of the cooperation program with the Russian Federation.

[1] See, for example, B. Chu, *Laser Light Scattering: Basic Principles and Practice* (Academic Press, San Diego, 1991).
[2] S. Dierker, NSLS Newsletter, July, 1995; D. L. Abernathy *et al.,* J. Synchrotron Radiat. **5**, 37 (1998); B. Lengeler, Naturwissenschaften **88**, 249 (2001).
[3] S. Brauer *et al.,* Phys. Rev. Lett. **74**, 2010 (1995); S. B. Dierker, R. Pindak, R. M. Fleming, I. K. Robinson, and L. Berman, Phys. Rev. Lett. **75**, 449 (1995).
[4] S. G. J. Mochrie *et al.,* Phys. Rev. Lett. **78**, 1275 (1997); O. K. C. Tsui and S. G. J. Mochrie, Phys. Rev. E **57**, 2030 (1998); T. Thurn-Albrecht *et al.,* Phys. Rev. E **59**, 642 (1999); L. B. Lurio *et al.,* Phys. Rev. Lett. **84**, 785 (2000); D. O. Riese *et al.,* Phys. Rev. E **61**, 1676 (2000); G. Grübel, D. L. Abernathy, D. O. Riese, W. L. Vos, and G. H. Wegdam, J. Appl. Crystallogr. **33**, 424 (2000); D. Lumma, L. B. Lurio, M. A. Borthwick, P. Falus, and S. G. J. Mochrie, Phys. Rev. E **62**, 8258 (2000); T. Seydel, A. Madsen, M. Tolan, G. Grübel, and W. Press, Phys. Rev. B **63**, 073409 (2001); J. Lal, D. L. Abernathy, L. Auvray, O. Diat, and G. Grübel, Euro. Phys. J. E **4**, 263 (2001).
[5] A. C. Price *et al.,* Phys. Rev. Lett. **82**, 755 (1999).
[6] A. Fera *et al.,* Phys. Rev. Lett. **85**, 2316 (2000).
[7] See, for example, P. M. Chaikin and T. C. Lubensky, *Principles of Condensed Matter Physics* (Cambridge University Press, Cambridge, England, 1995).
[8] See, for example, P. Pieranski *et al.,* Physica (Amsterdam) **195A**, 364 (1993); A. A. Sonin, *Freely Suspended Liquid Crystalline Films* (Wiley-VCH Verlag GmbH, Berlin, Germany, 1998).
[9] J. C. Earnshaw, Appl. Opt. **36**, 7583 (1997).
[10] R. Holyst, Phys. Rev. A **44**, 3692 (1991); A. N. Shalaginov and V. P. Romanov, Phys. Rev. E **48**, 1073 (1993).
[11] A. N. Shalaginov and D. E. Sullivan, Phys. Rev. E **62**, 699 (2000).
[12] A. Poniewierski, R. Holyst, A. C. Price, and L. B. Sorensen, Phys. Rev. E **59**, 3048 (1999); H.-Y. Chen and D. Jasnow, Phys. Rev. E **61**, 493 (2000); V. P. Romanov and S. V. Ul'yanov, Phys. Rev. E **63**, 031706 (2001).
[13] S. Gierlotka, P. Lambooy, and W. H. de Jeu, Europhys. Lett. **12**, 341 (1990); D. J. Tweet, R. Holyst, B. D. Swanson, H. Stragier, and L. B. Sorensen, Phys. Rev. Lett. **65**, 2157 (1990); E. A. L. Mol, G. C. L. Wong, J. M. Petit, F. Rieutord, and W. H. de Jeu, Phys. Rev. Lett. **79**, 3439 (1997).
[14] E. A. L. Mol, J. D. Shindler, A. N. Shalaginov, and W. H. de Jeu, Phys. Rev. E **54**, 536 (1996).
[15] A. Q. R. Baron, Hyperfine Interact. **125**, 29 (2000).